ORIGINAL ARTICLE

Journal of Cachexia, Sarcopenia and Muscle 2022; **13**: 1403–1417
Published online 17 February 2022 in Wiley Online Library (wileyonlinelibrary.com) **DOI:** 10.1002/jcsm.12938

Role of skeletal muscle satellite cells in the repair of osteoporotic fractures mediated by β-catenin

Zhenxiong Jin[1,2,3†], Weiwei Da[1,2†], Yongjian Zhao[1,2†], Tengteng Wang[1], Hao Xu[1,2], Bing Shu[2,3], Xiang Gao[4], Qi Shi[1,2], Yong Ma[5], Yan Zhang[1,2*], Yongjun Wang[2,3*] & Dezhi Tang[1,2*]

[1]*Longhua Hospital, Shanghai University of Traditional Chinese Medicine, Shanghai, China;* [2]*Institute of Spine, Shanghai University of Traditional Chinese Medicine, Shanghai, China;* [3]*Shanghai University of Traditional Chinese Medicine, Shanghai, China;* [4]*Department of Orthopedics, Huadong Hospital Affiliated to Fudan University, Shanghai, China;* [5]*Department of Orthopedics, Hospital Affiliated to Nanjing University of Traditional Chinese Medicine, Nanjing, Jiangsu, China*

Abstract

Background Osteoporosis is a metabolic disease, and osteoporotic fracture (OPF) is one of its most serious complications. It is often ignored that the influence of the muscles surrounding the fracture on the healing of OPF. We aimed to clarify the role of skeletal muscle satellite cells (SMSCs) in promoting OPF healing by β-catenin, to improve our understanding of SMSCs, and let us explore its potential as a therapeutic target.

Methods Skeletal muscles were obtained from control non-OPF or OPF patients for primary SMSCs culture (n = 3, 33% females, mean age 60 ± 15.52). Expression of SMSCs was measured. *In vivo*, 3-month-old female C57BL/6 mice underwent OVX surgery. Three months later, the left tibia fracture model was again performed. The control and the treatment group (n = 24, per group, female). The treatment group was treated with an agonist (osthole). Detection of SMSCs in muscles and fracture healing at 7, 14, and 28 three time points (n = 8, 8, 8, female). To further clarify the scientific hypothesis, we innovatively used Pax7-Cre$^{ERT2/+}$;β-catenin$^{fx/fx}$ transgenic mice (n = 12, per group, male). Knock out β-catenin in SMSC to observe the proliferation and osteogenic differentiation of SMSCs, and OPF healing. *In vitro* primary cells of SMSCs from 3-month-old litter-negative β-catenin$^{fx/fx}$ transgenic mice. After adenovirus-CRE transfection, the myogenic and osteogenic differentiation of SMSC was observed.

Results We find that human SMSCs reduced proliferation and osteogenic differentiation in patients with OPF (−38.63%, $P < 0.05$). And through animal experiments, it was found that activation of β-catenin promoted the proliferation and osteogenic differentiation of SMSC at the fracture site, thereby accelerating the healing of the fracture site (189.47%, $P < 0.05$). To prove this point of view, in the *in vivo* Pax7-Cre$^{ERT2/+}$;β-catenin$^{fx/fx}$ transgenic mouse experiment, we innovatively found that knocking out β-catenin in SMSC will cause a decrease in bone mass and bone microstructure, and accompanied by delayed fracture healing (−35.04%, $P < 0.001$). At the same time, through *in vitro* SMSC culture experiments, it was found that their myogenic (−66.89%, $P < 0.01$) and osteogenic differentiation (−16.5%, $P < 0.05$) ability decreased.

Conclusions These results provide the first practical evidence for a direct contribution of SMSCs to promote the healing of OPF with important clinical implications as it may help in the treatment of delayed healing and non-union of OPFs, and mobilization of autologous stem cell therapy in orthopaedic applications.

Keywords Skeletal muscle stem cells; Osteoporotic fracture; Osteoblast; β-Catenin

Received: 11 May 2021; Revised: 8 January 2022; Accepted: 17 January 2022
**Correspondence to: Dezhi Tang and Yan Zhang, Longhua hospital, Institute of Spine, Shanghai University of Traditional Chinese Medicine, 725 Wan-Ping South Road, Shanghai 200032, China. Fax: +86 216443 4704. Email: dztang702@126.com; medicineyan@aliyun.com; Yongjun Wang, Shanghai University of Traditional Chinese Medicine, 1200 Cailun Road, Shanghai 201203, China. Fax: +86 216443 4704. Email: yjwang8888@126.com*
† These authors contributed equally to this article.

Introduction

Osteoporotic fracture (OPF) is a serious health problem worldwide. Upset the balance between bone formation of osteoblasts and bone resorption by osteoclasts, leading to the deterioration of the bone structure, thereby increasing the risk of fractures in patients.[1] According to statistics, about 200 million women worldwide suffered from osteoporosis, and its prevalence has risen from 4% among women aged 50–59 years to 52% among women aged more than 80 years.[2] Simultaneously, the risk of subsequent fracture increases.[3] Common sites of osteoporotic bones are often comminuted and compromised, making it difficult to achieve optimal healing results.[4] When a fracture occurs, surgery is the main treatment strategy for OPFs.[5] However, patients' age, physique, and surgical factors all lead to a poor prognosis and complications.[6] Whenever a fracture occurs, doctors focus on the influence of bone marrow mesenchymal stem cells in the bone marrow cavity on fracture healing and often ignore the influence of muscles around the fracture site and muscle-derived stem cells on fracture healing.

Skeletal muscle satellite cells (SMSCs) adhere to the muscle fibres and are located between the sarcolemma and the basement membrane.[7] They are normally in a relatively static state but can show pluripotent mesenchymal stem cell activity after stimulation.[8] Pax7 is an important molecular marker for muscle satellite cells and determines satellite cell formation during embryonic development.[9] Also, several proteins of the myocyte enhancement factor 2 (MEF2) family and many muscle-derived regulators, such as myogenic differentiation 1 (MyoD1) and myogenic factor 5 (Myf5), have been reported.[10] SMSCs isolated from injured skeletal muscle fibres can differentiate into osteoblasts without osteoinductive agents.[11] Besides, a more recent investigation of semaphoring 3A secreted by activated SMSCs can balance the effects of bone formation and bone remodelling.[12] These results indicated that SMSCs also could differentiate into osteoblasts, but reports on this are rare, and the specific signalling pathways mediated to this stage of osteogenesis are not clear.

β-Catenin signalling regulates a wide range of physiological processes as key pathways, including cell proliferation and migration.[13] In adult muscle regeneration, the activation and proliferation of SMSCs are associated with Wingless/integrated (Wnt) activation and nuclear localization of β-catenin.[14] β-Catenin with downstream Tcf/Lef interactions is recurring during damage-induced reactivation.[15] Moreover, β-catenin signalling is most likely to change due to genetic and/or epigenetic factor(s) in patients with muscle defects such as myopathies and atrophy.[16] In particular, the up-regulation of MyoD enhanced the chemoresistance of the cell by elevating β-catenin activity.[17] Mechanistically, the β-catenin cascade represents the classic Wnt pathway and is important in various biological activities of stem cells.[18] Furthermore, some scholars found that a precise level of β-catenin activity is essential for regulating the amplification and differentiation of satellite cell descendants during adult myogenesis.[14,19] In the selection of β-catenin agonists, our previous research found that osthole can stimulate osteoblast differentiation and bone formation by activation of β-catenin.[20] Osthole is a natural coumarin first derived from the *Cnidium* plant.[21] Recently, osthole has received increasing attention due to its active ingredients in the prevention of osteoporosis. Osthole exhibited a good safety profile and biological uses compared with other agonists products.[22]

In this present study, we verified the role of SMSCs in the healing of OPFs through several steps, and the β-catenin signalling pathway plays a crucial role in the healing of OPFs. First, it was found that the proliferation and osteogenic differentiation of human SMSC (hSMSC) in OPF patients were reduced. Secondly, using OVX mice *in vivo* experiments to find that promoting the expression of SMSC and β-catenin can accelerate fracture healing. Third, using Pax7-Cre$^{ERT2/+}$;β-catenin$^{fx/fx}$ mice to knock out β-catenin in SMSC, we found that the mice showed significant bone loss and delayed fracture. Finally, through the *in vitro* osteogenic and myogenic differentiation studies of conditionally knocking out β-catenin in SMSCs, it was once again confirmed.

Materials and methods

Human skeletal muscle satellite cell isolation

The human skeletal muscles samples were aseptically obtained from two patients with OPFs and one patient with normal fractures in the operating room of Longhua Hospital. Each skeletal muscle sample was extracted to a size of approximately 1*1*0.5 cm. The samples were put in Hanks' balanced salt solution (HBSS) (Gibco, 14025-076, USA) + 2% penicillin–streptomycin (PS) (Biosera, XC-A4122/100, France) and carried to the laboratory in Taichung. Then, 0.2% Col II digestive enzyme was added, and the samples were digested in a cell culture incubator at 37°C. Repeated pipetting was done, and incubation was continued. Then, centrifugation was performed. The supernatant was removed, 1 mg/mL dispase (grade II, 8 U) was added, and the cell cultures were incubated. After repeated pipetting, the suspension was filtered through 100, 70, and 40 μm sieves in order and centrifuged. The supernatant was removed. Subsequently, NH_4CL (2 mL) was added to resuspend the cells and mixed by pipetting. The red blood cells will lyse and float in the supernatant at room temperature, centrifuge, and remove the supernatant. Then, cell culture solution [Dulbecco's modified Eagle's medium (DMEM) (Biosera, LM-D1110/500, France) + 20% foetal bovine serum (FBS) + 10% horse serum + 0.5% chicken em-

bryo extract + 1% PS] was added, and the cells were resuspended. Subsequently, the cells were inoculated into a 10 cm Petri dish. After 2 h of culture, the non-adherent cells were transferred to a new culture dish (PP2 generation), a new medium was added to the culture, and the solution was changed every 2–3 days.

Alkaline phosphatase staining

The cells were rinsed with PBS three times. Next, 2 mL of 10% neutral formalin was added and fixed. The cells were rinsed with PBS three times, followed by the addition of 1.5 mL of one-step nitro-blue tetrazolium chloride/5-bromo-4-chloro-3′-indolyl phosphate p-toluidine salt (Thermo, 34042, USA). The specific method follows the instructions.

Real-time PCR analysis in vitro

The cells were inoculated in six-well plates. Then, 10^{-4}, 10^{-5}, 10^{-6}, and 10^{-7} M snake bed fluid working solution was added. Then, 1 mL of TRIzol (Invitrogen, USA) was added. The specific method follows the instructions. Chloroform (200 μL) was added. Centrifuge to the supernatant was taken after centrifuge, and an equal volume of isopropanol was added. Then, 1 mL of 75% ethanol was added after centrifuge again. The supernatant was removed and dried. Then, DEPC water (30 μL) was added and mixed by pipetting. Using a Takara reverse transcription kit (Takara, RR037A, JPN) following the manufacturer's protocol. RT-PCR was performed for related osteogenic genes. The sequence number of the gene of interest was found in PubMed-Primer-Blast, and then the primers were designed for Big Co., Ltd. (Beijing Liuhe, China). RT-PCR was used to measure gene expression. The following primer sets were used (all sequences 5′–3′): Col I-F, CTGGCCTCCCTGGAATGAAG; Col I-R, GGACCTTCAGAGCCTCGGG; Runx2-F, AACCCACGAATGCACTATCCA; Runx2-R, CGGACATACCGAGGGACATG; BMP2-F, TCCATGTGGACGCTCTTTCAA; BMP2-R, AAGCAGCAACGCTAGAAGACA; Osteocalcin-F, AGCAAAGGTGCAGCCTTTGT; Osteocalcin-R, GCGCCTGGGTCTCTTCACT; Axin2-F, ACTGCCCACACGATAAGGAG; Axin2-R, CTGGCTATGTCTTTGGACCA; ALP-F, CCGTGGCAACTCTATCTTTGG; and ALP-R, GCCATACAGGATGGCAGTG. Relative quantification was performed by the $2^{-\Delta\Delta Ct}$ method, using β-actin as the reference gene.[23]

Mouse experiments

A total of 48 two-month-old sun protection factor-grade C57BL/6 mice were purchased from the Institute of Zoology, Chinese Academy of Sciences and raised to 12 months of age. All animals had free access to water and food throughout the experiment. All 48 mice were numbered 1–48 using the toe-clipping method. After 12 months, their average weight was 40 g. The β-catenin$^{fx/fx}$ and Pax7 Cre$^{ERT2/+}$ mice were generated as previously described and maintained on C57BL/6J background. Pax7 Cre$^{ERT2/+}$ mice were crossed with β-catenin$^{fx/fx}$ mice to obtain Pax7 Cre$^{ERT2/+}$;β-catenin$^{fx/fx}$ mice (C57BL/6J). Genetic identification was performed at the 3-week-old age. Mouse genotypes were determined by PCR on tail genomic DNA. Primer sequences were available upon request. They were randomly divided into the Pax7 Cre$^{ERT2/+}$;β-catenin$^{fx/fx}$ group and the β-catenin$^{fx/fx}$ group. Each group had two time points 7 and 14 dpf, with 12 mice in each group at each time point. For postnatal activation of Pax7 Cre, 100 mg/kg tamoxifen (Sigma, T5648, USA) in corn oil was intraperitoneally injected into 1-month-old mice once a day for five consecutive days. The animal protocols were reviewed and approved by the Shanghai University of traditional Chinese medicine on animal care (Ethics Review Number: PZSHUTCM190329005) and conformed to the National Institutes of Health Guide for the Care and Use of Laboratory Animals.

Building a fracture model

First, 12-month-old C57BL/6 mice and 3-month-old Pax7-CreER;β-catenin$^{fx/fx}$ mice were anaesthetized intraperitoneally with ketamine hydrochloride. The mice were placed in the supine position. Hair from their calf was removed and disinfected with iodine, and the skin was cut 1.5 cm through the left anterior tibia under aseptic conditions. Second, the fascia and muscles on the medial and lateral parts of the upper tibia were bluntly separated. The Kirschner wire was inserted from the tibial plateau into the upper one-third of the tibia. Then, the tibia was completely transected. A Kirschner wire was inserted into the bone cavity at the lower end of the broken end, and the part that leaked out of the bone was cut off. Finally, the skin was sutured layer by layer.

Drug formulation

C57BL/6 were administered osthole at a concentration of 5 mg/(kg·day); the maximum dose capacity was 60 μL/day. In the pharmacopoeia, the maximum daily dose of osthole was 9 g, which was equivalent to 0.13 g/(kg·day) based on 70 kg human weight, and the configured concentration was 5 g/mL. The formula for calculating the total amount of osthole element = 5 mg/(kg·day) × 10^{-3} × weight g × day × *N* (number). The formula for calculating the total amount of corn oil = 60 μL × *N* (number) × day. First, osthole was dissolved in an appropriate amount of dimethyl sulfoxide and mixed by pipetting. After osthole was completely dissolved, corn oil was added to it to prepare an injection. The drug intervention method was as follows. All mice received

drug intraperitoneal (IP) injection on the second day after surgery, 60 μL intraperitoneally. The mice in the osthole group were injected with osthole, while those in the vehicle group were injected with corn oil. All mice had free access to water.

Micro-computed tomography

The left tibia was immediately removed. And it was immersed in 10% neutral formalin for 24 h. The formalin was replaced with 75% ethanol for long-term fixation, and a micro-computed tomography (CT) scan was performed for uniform positioning. The left upper tibia was one-third, and the resolution was 18 μm. Quantitative analysis of bone tissue morphology was performed, including BV/TV, the number of trabecular bone (Tb. N), thickness of trabecular bone (Tb. Th), trabecular bone separation (Tb. Sp), and bone density (mean/density of TV, mean/density of BV).

After 28 days, the fracture site of each group was scanned by micro-CT. The biomechanical analysis was performed using finite element software, including stiffness, apparent modulus Ezz, failure load estimate, and cross-sectional area.

Histopathological observation of tibial fractures

Use 14% ethylenediaminetetraacetic acid (pH 7.4) was applied for decalcification for 3–4 weeks. After confirming the decalcification by X-ray, dehydration and paraffin embedding were performed, and sagittal serial sections (4 μm) were performed. Decalcified femoral sections were stained with haematoxylin and eosin (HE) and Alcian Blue/Haematoxylin and Orange G (ABHO), collected, and analysed using Olympus VS120-SL.

Real-time PCR analysis in vivo

The following primer sets were used (PubMed-Primer-Blast ID): Col-1 (NM_007743.3); Pax7 (NM_011039.2); Runx2 (NM_001146038.2); BMP2 (NM_007553.3); Osteocalcin (OC) (NM_007541.3); Engrailed 1 (EN1) (NM_010133.2); AXIN2 (NM_015732.1); Osteopontin (OPN) (NM_001204201.1); AXIN1 (NM_001159598.2); TCF1 (NM_009331.1); MYOD1 (NM_010866.1); Myogenin (NM_031189.1); and Myf5 (NM_008656.1). Relative quantification was determined by the $2^{-\Delta\Delta Ct}$ method using β-actin as the reference gene[23] (Supporting Information, *Table* S1).

Immunohistochemical staining

Briefly, after routine dewaxing, the sections were immersed in methanol : H_2O_2 (1:9) for 15 min, and then antigen retrieval was carried out with 0.1% collagenase from *Clostridium perfringens* (Sigma, c6885, USA) in a 37°C thermostat for 30 min. The sections were blocked with 5% BSA at room temperature for 20 min. Primary rabbit antibodies were used to visualize β-catenin (Abcam, ab6302, USA; β-catenin : 1% BSA 1:200)/Runx2 (Abcam, ab23981, USA; Runx2 : 1% BSA 1:200), overnight at 4°C. Goat anti-rabbit IgG (Abcam, ab205718) was added dropwise and incubated at 37°C for 15 min. Avidin/Biotin enzyme complex-horseradish peroxidase (Vectorlabs, PK-6100, USA) was added dropwise at room temperature for 15 min. Then, the 3,3′-diaminobenzidine (Vectorlabs, SK-4100, USA) colour development solution was used, and Olympus VS120-SL 20x eyepiece was used for observation.

Immunofluorescent staining

In short, after routine dewaxing, antigen retrieval was carried out with 0.1% collagenase from *C. perfringens* (Sigma, c6885, USA) in a 37°C thermostat for 30 min. The sections were blocked with 5% BSA at room temperature for 20 min. Primary rabbit antibodies were used to visualize Pax7 (Abcam, ab187339, UK; Pax7 : 1% BSA 1:200) + BrdU (Abcam, ab6326, UK; BrdU : 1% BSA 1:200); MyoD (Abcam, ab133627, UK; MyoD : 1% BSA 1:200) + BrdU (Abcam, ab6326, UK; BrdU : 1% BSA 1:200); Pax7 (Abcam, ab187339, UK; Pax7 : 1% BSA 1:200) + Sca1 (Abcam, ab25031, UK; Sca1 : 1% BSA 1:200), overnight at 4°C. Anti-rabbit IgG [Cell Signaling Technology (CST) 4412, USA, 488; 488 : 5% BSA 1:500 + CST 4413/4409, USA, 555, 555 : 5% BSA 1:500] was added. The cells were protected from light and maintained at room temperature for 1 h. The nuclei were counterstained with DAPI (Vectorlabs, H-1200-10, USA). An Olympus VS120-SL 20-fold filter (green, blue, and ultraviolet) was used to image samples, and three colours were synthesized.

Statistical analysis

All data were presented as mean ± standard error of the mean. The sample sizes were calculated assuming that a 30% difference in the parameters measured would be considered biologically significant with an estimate of sigma of 10–20% of the expected mean. Alpha and beta were set to the standard values of 0.05 and 0.8, respectively. No animals or samples were excluded from the analysis, and animals were randomized to treatment versus control groups, where applicable. For relevant data analysis, first, the normality plots were performed with tests for checking normal distributions of the groups. For comparison between the two sets of data, an independent sample *t*-test was used to meet the normal distribution. If normality tests failed, the Mann–Whitney tests were then used for comparisons be-

tween the two groups. For comparisons of three or four groups, the one-way analysis of variance and least-significant difference test was used if the data passed the normality tests; otherwise, the Kruskal–Wallis test was used, followed by Dunn's multiple comparison test. The SPSS 24.0 statistical software was used for statistical analysis. A P value < 0.05 was considered statistically significant ($^*P < 0.05$; $^{**}P < 0.01$; and $^{***}P < 0.001$). The GraphPad Prism 8 was used as the drawing software.

Results

Patients with osteoporotic fracture had reduced human skeletal muscle satellite cells proliferation and weakened osteogenic differentiation

First, the diagnosis of OPF or non-OPF was confirmed based on the radiographs, dual-energy X-ray absorptiometry, and clinical data. The muscles were collected intraoperatively. Flow cytometry revealed that the positive expression rate of hSMSCs (CD90+ and CD56+) was 12.8% in patients with non-OPFs and 78.1% in patients with OPFs (*Figure* S1A and S1B). However, Pax7 and 5-Bromo-2-deoxyUridine (BrdU) in hSMSCs were double fluorescent immunostained. The results showed that the number of cells was significantly less in the OPF group than in the normal fracture group. The difference in positive expression between the normal fracture group and the OPF group was statistically significant ($^*P < 0.05$; *Figure* 1A and 1B). Then, alkaline phosphatase (ALP) staining was performed in hSMSCs, which was more pronounced in patients with normal fractures than in those with OPFs. ALP expression was significantly reduced in the OPF group compared with the non-OPF group ($^*P < 0.05$; *Figure* 1C and 1D). Finally, the quantitative real-time reverse transcription-polymerase chain reaction (RT-PCR) results of hSMSC-related genes in patients with normal fractures and OPFs were obtained. The expression of bone morphogenetic protein 2 (BMP2) and runt-related transcription factor 2 (Runx2) was significant in the normal fracture group compared with the OPF group ($^*P < 0.05$; *Figure* 1E and 1F). Also, the proliferation of hSMSCs and β-catenin expression decreased in patients with OPFs ($^{***}P < 0.001$; *Figure* 1G and 1H).

Regarding the choice of therapeutic drugs, we found through *in vitro* experiments that osthole has a better curative effect. Different concentrations of osthole (10^{-4}, 10^{-5}, and 10^{-6} M) were formulated and made to interfere with hSMSCs for 3 days, and Pax7 and BrdU immunofluorescence double staining was performed (*Figure* S1C). Osthole (10^{-6} M) was significantly different from the control, indicating that osthole could promote the activity of hSMSCs ($^*P < 0.05$; *Figure* S1D). Afterward, RT-PCR detection of the expression of BMP2, ALP, collagen type 1 (COL1), and Runx2 was performed. These genes were related to the osteogenic differentiation of cells. The results showed that 10^{-6} M osthole could promote the expression of BMP2, ALP, COL1, and Runx2 significantly in hSMSCs, with statistically significant differences ($^*P < 0.05$; *Figure* S1E–S1H). It shows that osthole may promote the osteogenic differentiation of SMSCs.

Activate the proliferation and osteogenic differentiation of skeletal muscle satellite cells, and up-regulate the expression of β-catenin, which can promote the healing of osteoporotic fracture

Three-month-old female C57BL/6 mice underwent OVX surgery. Three months later, the left tibia fracture model was again performed. The treatment group was given osthole, and the control group was given equal metering oil. Observe the changes of various indicators on the 7, 14, and 28 days post-fracture (dpf). The immunohistochemical staining of the fracture site and skeletal muscle with β-catenin showed that osthole promoted the expression of β-catenin in skeletal muscle and callus near the fracture point of OPF in mice (*Figure* 2A). Immunofluorescence double staining of muscle stem cell-specific protein gene Pax7 + BrdU was performed. The expression of Pax7 + BrdU was significantly higher in the treatment group than in the control group at 7/14/21 dpf. The expression of Pax7 was only found in the control group, and no expression of BrdU was observed. This finding showed that osthole could promote the proliferation of muscle-derived stem cells (*Figure* 2B–2D). This indicates that osthole can promote the expression of β-catenin in skeletal muscle and promote the proliferation and differentiation of SMSCs. For further confirmation, we conducted *in vitro* experiments. It is found that osthole can also promote the β-catenin expression of SMSCs *in vitro* and promote the up-regulation of AXIN2. Axin2 was an important regulator of the Wnt/β-catenin signalling pathway and was involved in the regulation of cell proliferation, cell variability, and so on ($^*P < 0.05$; *Figure* S1I and S1J).

After, immunohistochemical staining for β-catenin was performed at the fracture site, and the extent of β-catenin-positive staining in the nucleus and cytoplasm was recorded. The findings showed that the treatment group showed results significantly different from those of the control group ($^*P < 0.05$; $^{**}P < 0.01$; *Figure* 2E and 2F). Furthermore, the Pax7 + Sca1 immunofluorescence staining was also performed in the callus of the fracture point of the left tibia at three time points of OPFs. The proliferation of SMSCs at the fracture site was higher in the treatment group than in the control group. The control group showed only the expression of Sca1 (*Figure* 2G–2I). This finding indicated that osteoblast

DOI: 10.1002/jcsm.12938

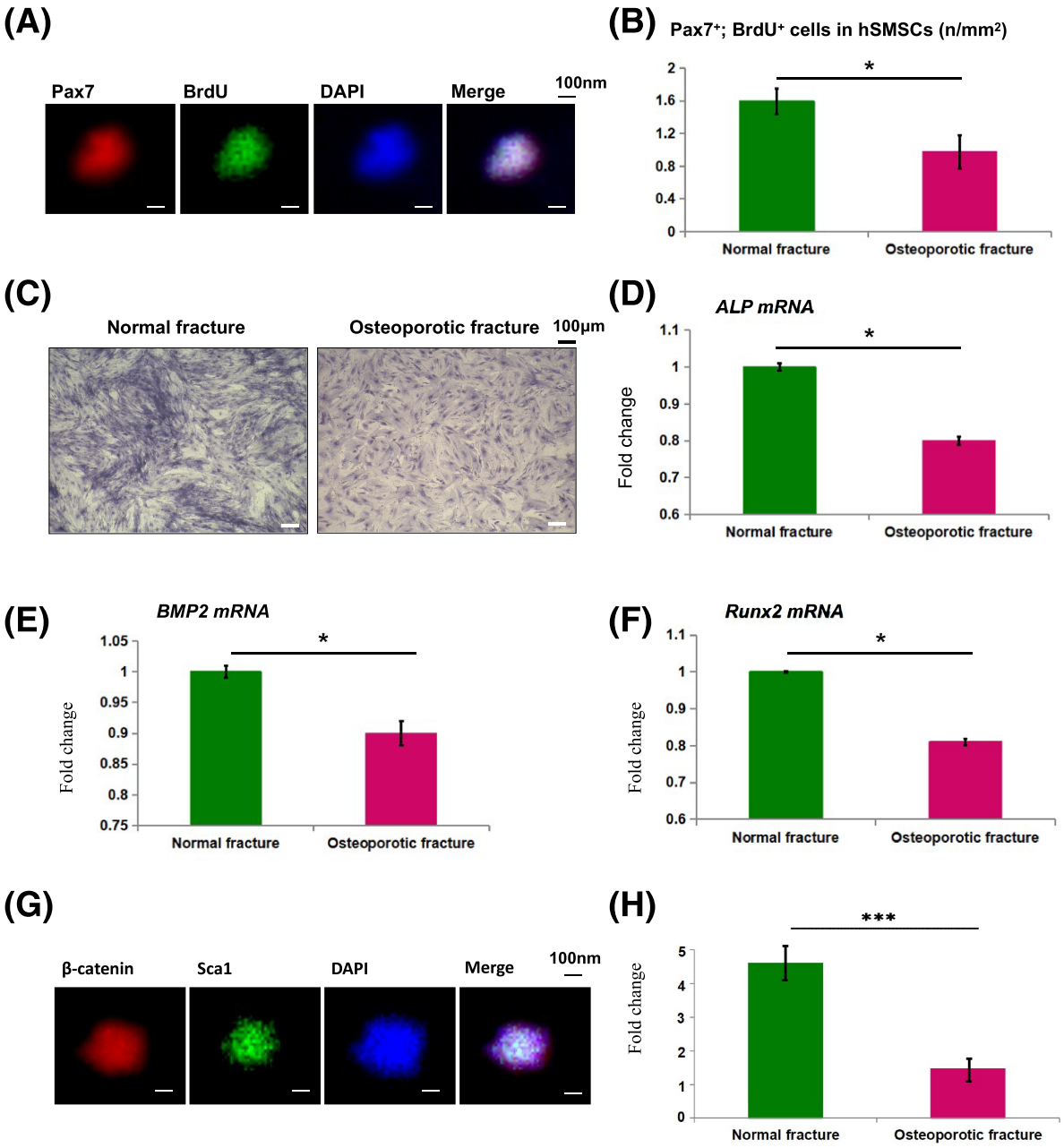

Figure 1 Patients with osteoporotic fracture (OPF) and having reduced proliferation of human skeletal muscle satellite cells (hSMSCs) and weakened osteogenic differentiation. *(A)* Double fluorescent immunostaining of Pax7 and BrdU in hSMSCs. *(B)* Five fields were randomly selected from each specimen under a microscope. The double staining positive cells were counted in the visual field. $*P < 0.05$, the positive expression of the normal fracture group was statistically different from that of the OPF group. The OPF group was significantly less than the normal fracture group. *(C)* ALP staining of hSMSCs in patients with non-OPF was more obvious than that of patients with OPF. *(D)* $*P < 0.05$, ALP was significantly reduced in the OPF group compared with the non-OPF group. The results of RT-PCR of hSMSCs related genes in patients with normal fracture and OPF. *(E)* $*P < 0.05$, significant expression of BMP2 in normal fracture group compared with OPF group. *(F)* $*P < 0.05$, there was a statistically significant difference in Runx2 between the OPF group and the normal fracture group. *(G)* Double immunofluorescence staining of β-catenin + Scal1 in hSMSC. *(H)* $***P < 0.001$, compared with the normal fracture group, the β-catenin + Scal1 double immunofluorescence staining in the OPF group was statistically significantly reduced.

could promote the migration of some SMSCs into the callus and accelerate fracture healing by mediating the β-catenin signal transduction pathway.

Through the micro-CT three-dimensional (3D) reconstruction of the fractured site and bone mass analysis, it was found that osthole could accelerate fracture healing

DOI: 10.1002/jcsm.12938

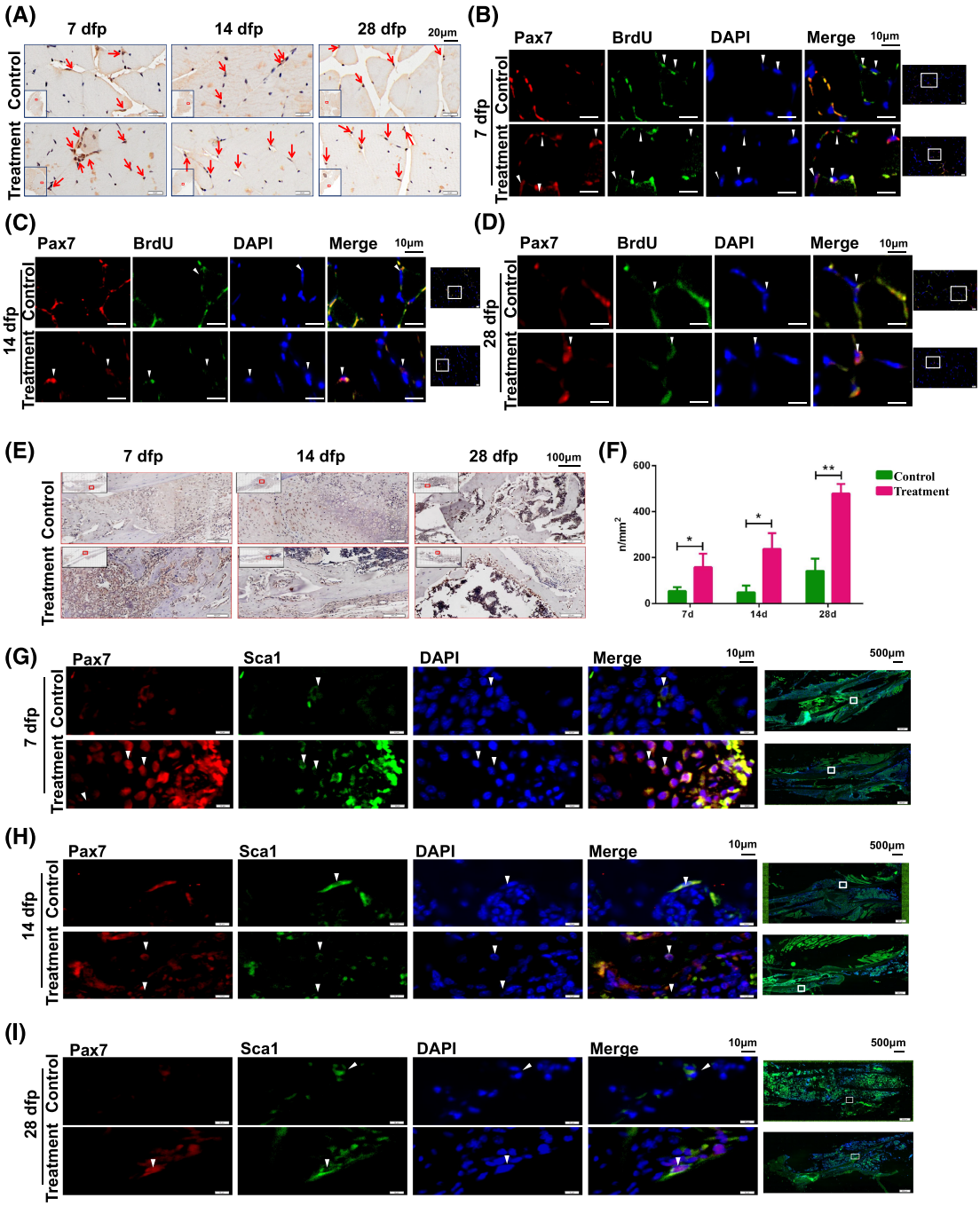

Figure 2 Drug intervention promotes the expression of β-catenin of SMSC, thereby promoting the proliferation and osteogenic differentiation of SMSC at the fracture site of OVX mice. Three-month-old female C57BL/6 mice underwent OVX surgery. Three months later, the left tibia fracture model was again performed. The control and the treatment group (n = 24, 24) at 7, 14, and 28 dpf (n = 8, 8, 8). The treatment group was treated with osthole. *(A)* β-Catenin staining of the left gastrocnemius muscle at 7, 14, and 28 dpf in the two groups of senile OPFs mice. Two groups of senile OPFs were stained with Pax7 + BrdU immunofluorescence at the 7th, 14th, and 28th dpf of the left gastrocnemius muscle. *(B)* The expression of Pax7 + BrdU was significantly higher in the treatment group at 7 dpf than in the control. *(C)* At 14 dpf, the treatment group could still promote the expression of a small amount of Pax7 + BrdU. *(D)* At 28 dpf, the treatment group could still promote the expression of an amount of Pax7 + BrdU. At 7, 14, and 28 dpf of senile OPF, the Pax7 + Sca1 immunofluorescence staining was observed in the callus of the fracture point of the left tibia. *(E)* Immunohistochemical staining of β-catenin in the fracture site: the number of β-catenin positive staining in the nucleus and cytoplasm. *(F)* $^{*}P < 0.05$ at 7 and 14 days, the expression of the treatment group was upper than that in the control. $^{**}P < 0.01$ at 28 days, the expression of the treatment group was significantly higher than that in the control. *(G)* The expression of SMSCs in the fracture site at 7 dpf was higher than that in the control. *(H)* The expression of the SMSCs-specific protein gene Pax7 in the fracture site of the treatment group at 14 dpf. *(I)* The expression of Pax7 + Sca1 in the fracture site at 28 dpf of the treatment group was observed.

DOI: 10.1002/jcsm.12938

(*$P < 0.05$; *Figure* S2A–S2D). Subsequently, a finite element analysis of the healing site of senile mice with OPF was performed at 28 dpf. The failure load and estimated cross-sectional area of the treatment group were significantly different from those of the control group, indicating that osthole could improve the biomechanical strength and fracture prognosis of OPFs (*$P < 0.05$; *Figure* S2E–S2G). The results of HE and ABHO staining showed that osteoblast could promote the activity of chondrocytes and osteoblasts in the early stage, thereby promoting intra-membrane and intra-chondral osteogenesis and accelerating fracture healing (*Figure* S2H and S2I). This result was further confirmed by performing Runx2 immunohistochemical staining at the fracture site (**$P < 0.01$; *Figure* S2J and S2K).

Conditional knockout β-catenin in skeletal muscle satellite cells, and decrease the ability of muscle proliferation and myogenic differentiation in Pax7-Cre$^{ERT2/+}$;β-catenin$^{fx/fx}$ mice

After breeding genetic mice, an agarose gel electrophoresis was performed at 3 weeks of age in newborn mice (*Figure* S3A). Pax7-Cre$^{ERT2/+}$;β-catenin$^{fx/fx}$ mice and littermate-negative β-catenin$^{fx/fx}$ transgenic mice were included in the study. At 4 weeks of age, all mice received tamoxifen injections for five consecutive days. When tamoxifen was administered bound to the ligand-binding region mutant, recognize loxp sites and exert Cre-recombinase activity to conditional knockout (cKO) genes. And the expression of β-catenin was tested at the age of 3 months. The muscle/body weight ratio of the two groups, the muscle coefficient of β-catenin$^{fx/fx}$ group was significantly higher than Pax7-Cre$^{ERT2/+}$;β-catenin$^{fx/fx}$ group (cKO group) (*$P < 0.05$; **$P < 0.01$; *Figure* 3A). Meanwhile, the Western blot analysis of the muscle showed that the expression level of β-catenin was significantly lower in the cKO group than in the β-catenin$^{fx/fx}$ group (***$P < 0.001$; *Figure* 3B). The same result can be observed by immunohistochemistry; the staining for β-catenin showed that the expression level of β-catenin in the cKO group was significantly lower than that in the β-catenin$^{fx/fx}$ group (***$P < 0.001$; *Figure* 3C). However, there was no difference in β-catenin staining of osteoblasts or their precursor cells in the knee, femur, and patella of the two groups (ns $P > 0.05$; *Figure* 3D and *Figure* S3B and S3C). Therefore, we can confirm that Pax7Cre$^{ERT2/+}$;β-catenin$^{fx/fx}$ conditional gene knockout mice only knock out β-catenin in SMSC. Through the HE staining of the muscle cross-section (*Figure* 3E) and the longitudinal section (*Figure* 3F) and Masson staining (*Figure* 3G), it can be observed that there is a significant muscle damage in the cKO group of mice.

Furthermore, RT-PCR analysis of the muscle showed that the expression levels of T cell factor-1 (TCF1), axin inhibitor (AXIN) 1, and AXIN2 were significantly lower in the cKO group than in the β-catenin$^{fx/fx}$ group. Besides, the expression of myogenic-related genes [Myf5, Myogenin, and myogenic differentiation 1 (MyoD1)] and the bone-related genes (Runx2, osteocalcin, osteopontin, and BMP2) in the β-catenin$^{fx/fx}$ group was significantly higher than that in the cKO group (*$P < 0.05$; **$P < 0.01$; ***$P < 0.001$; *Figure* 3H and *Figure* S3D). Immunofluorescence double staining was performed on the muscle. First, the results for MyoD + BrdU immunofluorescence double staining. The cKO group has decreased myogenic differentiation indicators (*Figure* 3I). Secondly, Pax7 + BrdU and Pax7 + Sca1 immunofluorescence double staining found that the proliferation and differentiation of SMSCs in the muscles of cKO group were reduced (*Figure* 3J and 3K).

Conditional knockout β-catenin in skeletal muscle satellite cells, thereby delaying the healing of tibial fractures in Pax7-Cre$^{ERT2/+}$;β-catenin$^{fx/fx}$ mice

Through the micro-CT detection of the tibia, it was found that the bone mass in the cKO group was significantly reduced (*Figure* 4A). The BMD, BV/TV, Conn-Dens, and Tb. N of the cKO group were significantly lower than the β-catenin$^{fx/fx}$ transgenic mice (**$P < 0.01$; *$P < 0.05$; *Figure* 4B). At the age of 3 months, the left tibia fracture model was again performed. It can be seen through the three-dimensional micro-CT reconstruction that the formation and remodelling of osteophytes were better in the cKO group than in the β-catenin$^{fx/fx}$ group at two time points (7 and 14 dpf) (*Figure* 4C). Followed by HE staining at 7 dpf, there was no osteophyte formation. At 14 dpf, β-catenin$^{fx/fx}$ group began to form callus (*Figure* 4C). Secondly, in ABHO staining at 7 dpf, there was no new bone formation, while, at 14 days, the β-catenin$^{fx/fx}$ group began to form a lot of new bone. The cKO group still does not affect new bone formation (*Figure* 4D). Because the callus of 7 dpf is not much different, a quantitative micro-CT analysis of 14 dpf is carried out and it is found that the BV/TV, Conn-Dens, Tb. N, and Tb. Sp expression in the cKO group was lower than that in the β-catenin$^{fx/fx}$ group at 14 dpf (**$P < 0.01$; ***$P < 0.001$; *Figure* 4F). This finding indicated that conditional knockout β-catenin in SMSCs, fracture healing was delayed. Immunohistochemical staining was also performed at the tibia fracture site. The extent of β-catenin-positive staining in the nucleus and cytoplasm in the cKO group was significantly different from that in the β-catenin$^{fx/fx}$ group (**$P < 0.01$; *Figure* 4G and 4H). Secondly, the extent of positive staining of Runx2 in the nucleus and cytoplasm was higher in the β-catenin$^{fx/fx}$ group than in the cKO group (*$P < 0.05$; *Figure* 4I and 4J). And in immunofluorescence staining of tibial fracture site (Pax7 + Sca1; Pax7 + BrdU), the positive expression of SMSCs in the cKO group was significantly lower than that in the β-catenin$^{fx/fx}$ group (*Figure* 4K; *Figure* S3E).

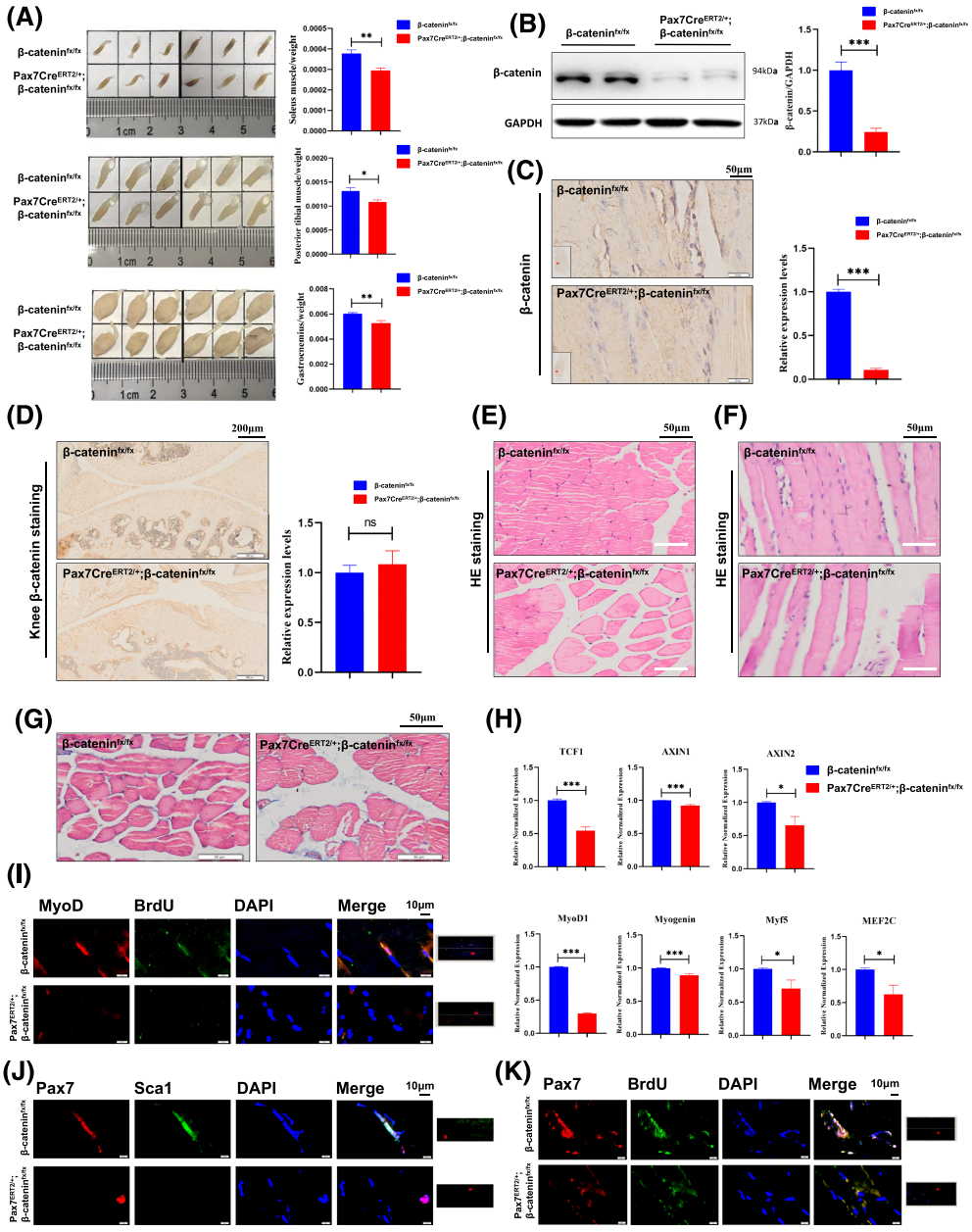

Figure 3 Knock out β-catenin in SMSC to observe the proliferation and osteogenic differentiation of muscle and SMSC in Pax7-Cre$^{ERT2/+}$;β-catenin$^{fx/fx}$ transgenic mice. Pax7-Cre$^{ERT2/+}$;β-catenin$^{fx/fx}$ transgenic mice and littermate-negative β-catenin$^{fx/fx}$ transgenic mice were injected with tamoxifen at the age of 1 month and were tested at the age of 3 months (n = 18, 18). *(A)* The muscle coefficient ratio of the two groups, the soleus muscle β-catenin$^{fx/fx}$ group was significantly higher than Pax7-Cre$^{ERT2/+}$;β-catenin$^{fx/fx}$ group, $^{**}P < 0.01$; the posterior tibial muscle Pax7-Cre$^{ERT2/+}$; β-catenin$^{fx/fx}$ group is lower than β-catenin$^{fx/fx}$ group, $^{*}P < 0.05$; the gastrocnemius β-catenin$^{fx/fx}$ group is significantly higher than Pax7-Cre$^{ERT2/+}$; β-catenin$^{fx/fx}$ group, $^{**}P < 0.01$; *(B)* Western blot analysis of muscle β-catenin knockout efficiency; *(C)* the β-catenin immunohistochemical staining of the left calf muscle of the two groups; *(D)* β-catenin staining of the knee joints. There is no statistical difference between the two groups, $P > 0.05$; *(E)* HE staining of left calf muscle of two groups of transgenic mice (cross-section); *(F)* HE staining of left calf muscle of two groups of transgenic mice (longitudinal section); *(G)* Masson staining of left calf muscles of two groups of transgenic mice. It can be seen that in the β-catenin$^{fx/fx}$ group, the muscles are very compact, but the Pax7-Cre$^{ERT2/+}$;β-catenin$^{fx/fx}$ group is still slack. *(H)* RT-PCR analysis of the posterior tibial muscle showed that in TCF1, AXIN1, and AXIN2, it was found that the Pax7-Cre$^{ERT2/+}$;β-catenin$^{fx/fx}$ group was significantly lower than the β-catenin$^{fx/fx}$ group, and after knocking out β-catenin in SMSCs, the expression of muscle-related genes Myogenin and MyoD1 was significantly reduced, $^{***}P < 0.001$; muscle-related genes Myf5 and MEF2C were reduced, $^{**}P < 0.05$; *(I)* immunofluorescence staining (MyoD + BrdU) of the posterior tibial muscle, the positive expression of MyoD in the Pax7-Cre$^{ERT2/+}$;β-catenin$^{fx/fx}$ group was significantly lower than that in the β-catenin$^{fx/fx}$ group, indicating that knockout β-catenin inhibits the proliferation of muscle cells, thereby delaying the repair of muscle damage. *(J)* Immunofluorescence staining (Pax7 + BrdU) of the posterior tibial muscle showed that the positive expression of SMSCs in the β-catenin$^{fx/fx}$ group was significantly higher than that of Pax7-Cre$^{ERT2/+}$;β-catenin$^{fx/fx}$ group. *(K)* Immunofluorescence staining (Pax7 + Sca1) of the posterior tibial muscle, the results are the same as above.

DOI: 10.1002/jcsm.12938

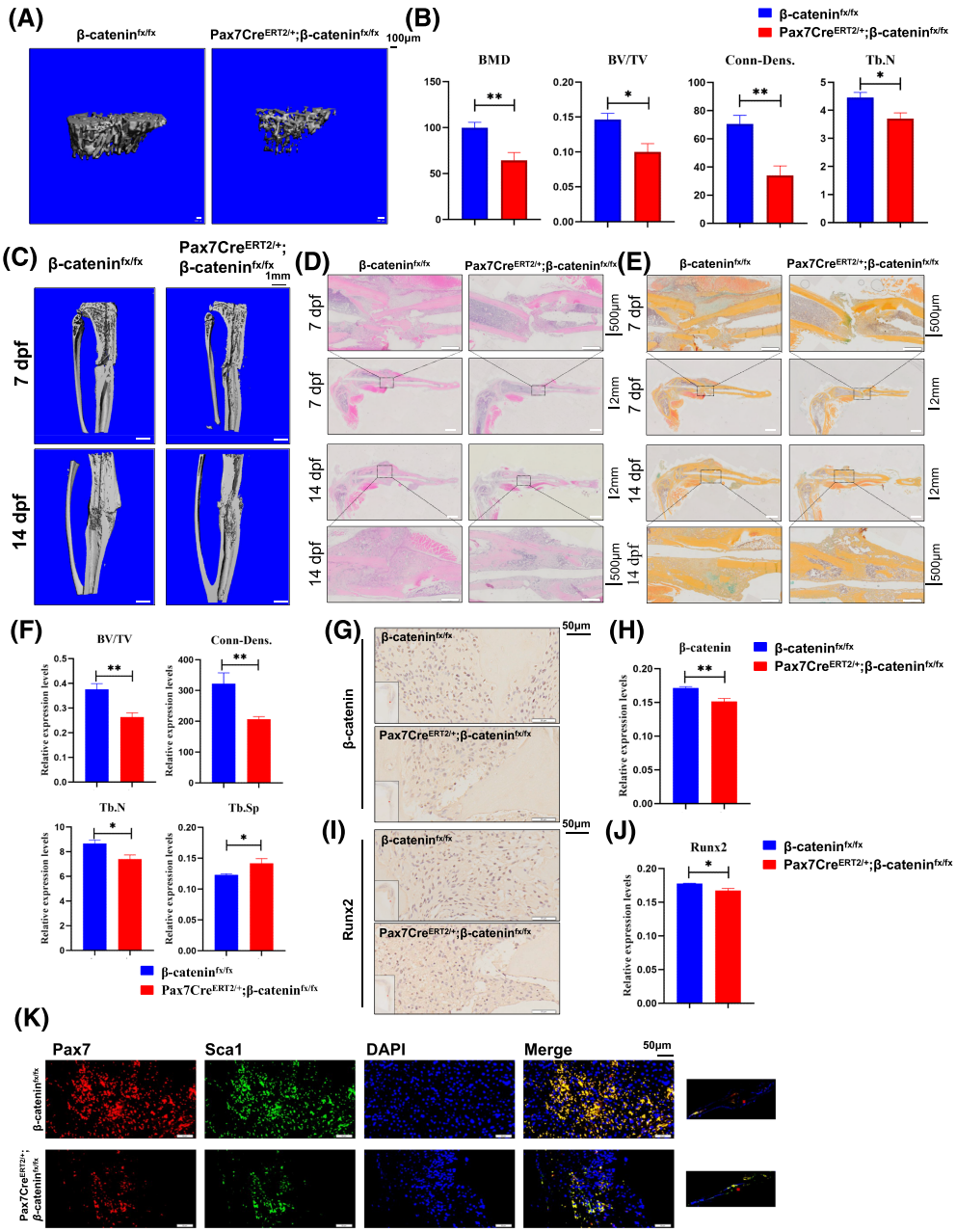

Figure 4 Knock out β-catenin in SMSC to observe the effect of Pax7-Cre$^{ERT2/+}$;β-catenin$^{fx/fx}$ mice on osteoporotic fracture healing. *(A)* Through the micro-CT detection of the tibia, it was found that Pax7-Cre$^{ERT2/+}$;β-catenin$^{fx/fx}$ transgenic mice decreased bone mass. *(B)* Pax7-Cre$^{ERT2/+}$;β-catenin$^{fx/fx}$ transgenic mice have significantly lower BMD than β-catenin$^{fx/fx}$ transgenic mice, $^{**}P < 0.01$; also, BV/TV, Conn-Dens, and Tb. N are also lower than β-catenin$^{fx/fx}$ transgenic mice, $^{*}P < 0.05$. At the 3 months old, surgery on the left tibia fracture (n = 12, 12). Each group had two time points: 7 and 14 dpf (n = 6, 6). *(C)* Micro-CT 3D reconstruction showed no significant difference at 7 dpf. At 14 dpf, the formation and remodelling of osteophytes in the Pax7-Cre$^{ERT2/+}$;β-catenin$^{fx/fx}$ group healed without the β-catenin$^{fx/fx}$ group. *(D)* HE staining: at 7 dpf, there was no osteophyte formation. At 14 dpf, β-catenin$^{fx/fx}$ transgenic mice group began to form callus. *(E)* ABHO staining: at 7 dpf, there was no new bone formation, while, at 14 days, the β-catenin$^{fx/fx}$ transgenic mice group began to form a lot of new bone. Pax7-Cre$^{ERT2/+}$;β-catenin$^{fx/fx}$ transgenic mice still do not affect new bone formation. *(F)* The micro-CT quantitative analysis of BV/TV, Conn-Dens, Tb. N, and Tb. Sp, at 14 dpf. The micro-CT analysis results showed that in the Pax7-Cre$^{ERT2/+}$;β-catenin$^{fx/fx}$ group, the BV/TV and Conn-Dens expression was lower than the β-catenin$^{fx/fx}$ group, $^{**}P < 0.01$; in contrast, the Tb. Sp of the Pax7-Cre$^{ERT2/+}$;β-catenin$^{fx/fx}$ group was larger than that of the β-catenin$^{fx/fx}$ group. *(G)* Immunohistochemical β-catenin staining: at 7 dpf, the fracture sites of each group were stained. *(H)* The number of β-catenin positive staining in the nucleus and cytoplasm of the β-catenin$^{fx/fx}$ group was different from that of the Pax7-Cre$^{ERT2/+}$;β-catenin$^{fx/fx}$ group, $^{*}P < 0.05$. *(I)* Immunohistochemical Runx2 staining: at 7 dpf, the fracture sites of each group were stained. *(J)* The number of positive staining of Runx2 in the nucleus and cytoplasm of the β-catenin$^{fx/fx}$ group was higher than that of the Pax7-Cre$^{ERT2/+}$; β-catenin$^{fx/fx}$ group, $^{**}P < 0.01$. *(K)* Immunofluorescence staining of tibial fracture site (Pax7 + Sca1), the positive expression of SMSCs in the Pax7-Cre$^{ERT2/+}$;β-catenin$^{fx/fx}$ group was significantly lower than that in the β-catenin$^{fx/fx}$ group.

DOI: 10.1002/jcsm.12938

In vitro *osteogenesis and myogenic differentiation of conditional knockout β-catenin in skeletal muscle satellite cells*

In vitro primary cells culture of SMSCs from the muscle tissue around tibia of 3-month-old litter-negative β-catenin$^{fx/fx}$ mice. After reaching 80% confluency, the cells were transfected with adenovirus (ad)-GFP and ad-CRE for 48 h, respectively. Observation of adenovirus transfection efficiency of cells by fluorescence microscope (*Figure* 5A). First, we use Western blot analysis to observe the differentiation of myogenesis and osteogenesis. The expression of β-catenin, Runx2, MEF2C, and Myogenin (MYOG) in the ad-CRE was significantly lower than that in the ad-GFP (*$P < 0.05$; **$P < 0.01$; ***$P < 0.001$; *Figure* 5B and 5C). Secondly, the expression of ALP in the ad-CRE was significantly lower than that in the ad-GFP (**$P < 0.01$; *Figure* 5D and 5E). And RT-PCR results showed that the TCF1, osteogenesis-related genes (Runx2, osteopontin, and Col1), and myogenic-related genes (MyoD, Myf5, and MEF2C) were also significantly lower than the ad-GFP group (**$P < 0.01$; *$P < 0.05$; *Figure* 5F). Finally, based on the two groups, the treatment group was treated with osthole and the control group was treated with DMSO, and ALP staining was observed (*Figure* 5G).

Discussion

This is the first report of an important regulatory role for SMSC in the repair of OPFs in which it maintains their differentiation into osteoblasts and restricts osteoclastogenesis mainly mediates the β-catenin signalling pathway. In middle-aged and elderly patients, the expression of SMSC in OPF patients is significantly lower than that in normal fracture patients, and β-catenin in SMSC is degraded, which prevents SMSC from maintaining its differentiation into osteoblasts, which limits bone formation. On the contrary, drug (osthole) intervention in OVX mice, while up-regulating β-catenin, promoted the osteogenic differentiation of SMSC and promoted the healing of OPFs. And using cKO mice, it was found that after knocking out the β-catenin in SMSC, the mice not only showed a significant reduction in bone mass and bone microstructure but also delayed fracture healing in compound fracture modelling. Consequently, (i) the proliferation of SMSCs in patients with OPFs is reduced and the osteogenic differentiation is weakened, and the activation of β-catenin in SMSC can promote the healing of OPFs; (ii) knocking out β-catenin in SMSC will cause bone loss, reduce the production of osteoblasts, and delay the healing of fractures (*Figure* 6).

The bone mass loss in 3-month-old cKO mice is fascinating, given that 9-month-old mice are osteoporotic. We attribute this to two functional changes in SMSCs due to β-catenin defects. First of all, muscle and SMSCs play a vital role in bone tissue engineering. SMSCs are responsible for postnatal muscle growth, regeneration, and homeostasis.[13,24,25] Following their discovery in 1961, it was speculated that SMSCs were dormant myoblasts and remained so until they were needed for skeletal muscle repair.[24,25] With aging, muscle tissue homeostasis is progressively disrupted and the ability of SMSCs to repair injured muscle markedly declines.[13,26] Also, undifferentiated muscle progenitor cells derived from a single satellite cell co-expressed multiple determination genes including those for MyoD and Runx2, which are specific for myogenic and osteogenic differentiation, respectively.[27] Remarkably, SMSCs can differentiate into osteogenic and chondrogenic lineages and have been shown to promote the repair of bone and cartilage.[28] MyoD is initially up-regulated in myogenic cells incubated with bone morphogenetic proteins (BMPs), suggesting that MyoD has a role in BMP-induced osteogenesis of myogenic cells.[29] The present study used Pax7-Cre$^{ERT2/+}$;β-catenin$^{fx/fx}$ mice; cKO mice's skeletal muscle myogenic-related indicators decreased, such as MyoD, MEF2C, and Myogenin; and the expression of Runx2 and BMP2 related to osteogenesis also decreased. The skeletal muscle healing in these mice was significantly worse than that in the control group, which again proved the aforementioned hypothesis. This finding suggested that other cell types with regenerative potential relied on the presence of SMSC populations and that these observations had considerable implications for bone-based and stem cell-based therapies.

Second, the β-catenin signalling pathway plays a crucial role in the proliferation and differentiation of osteoblasts. *In vivo*, animal experiments on cKO mice confirmed that knocking out β-catenin and inhibiting SMSCs led to delayed fracture healing. Moreover, previous studies have shown that osthole attenuates osteoclast formation by stimulating the activation of β-catenin-Osteoprotegerin (OPG) signalling and could be a potential drug for senile osteoporosis.[30] Furthermore, other signalling pathways have been reported to promote fracture healing in osteoporotic bone, such as epidermal growth factor receptor,[31] growth differentiation factor 11-fat mass, and obesity-associated protein axis.[32] Besides, oxidative stress and inflammation[33] might promote fracture healing, which requires in-depth exploration. These studies have opened a new chapter for the treatment of OPFs and provided a basis for future clinical applications.

Currently, OPFs and osteoporosis are common, particularly among older women, and hip fractures can be devastating.[34] In the USA, hip fracture rates and subsequent mortality among persons 65 years and older are declining, but comorbidities among patients with hip fractures have increased.[35] All types of hormone therapy studied confer substantial protection against fracture while they are used but wear off rapidly after use ceases.[36] Nonetheless, the use of these effective medications, which has been unsatisfactory in the

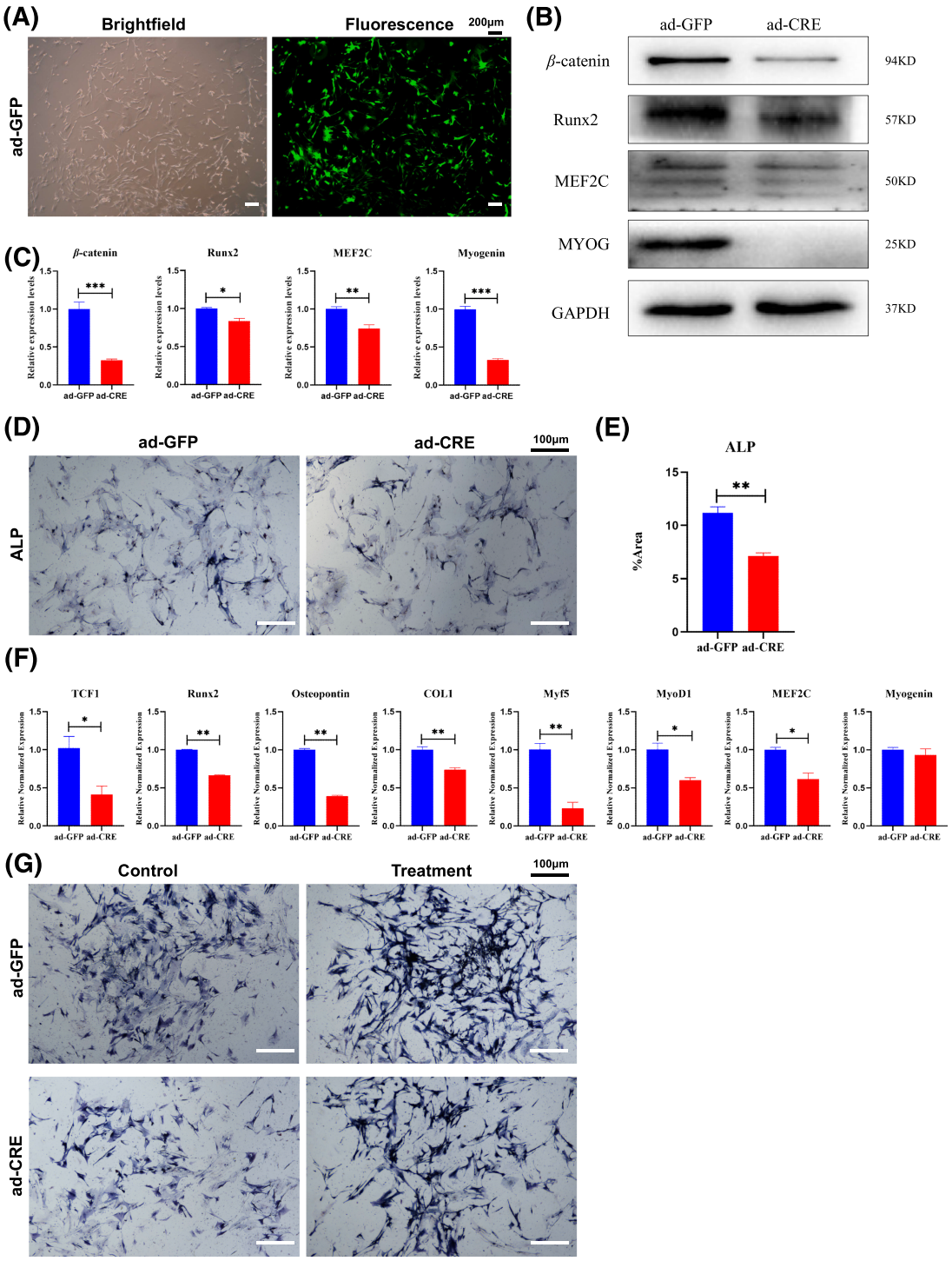

Figure 5 Osteogenesis and myogenic differentiation of β-catenin$^{fx/fx}$ transgenic mice *in vitro*. *In vitro* primary cells culture of SMSCs from the muscle group around tibia of 3-month-old litter-negative β-catenin$^{fx/fx}$ transgenic mice. *(A)* The cells grew to 80% and were transfected with ad-GFP and ad-CRE, respectively. Observe the virus transfection by fluorescence microscope after 48 h. *(B)* Western blot analysis of the SMSCs. *(C)* Western blot analysis of the posterior tibial muscle showed that the expression of β-catenin in the ad-CRE was significantly lower than that in the ad-GFP, $^{***}P < 0.001$; for Runx2, the ad-GFP was more than the ad-CRE, $^{*}P < 0.05$; for MEF2C, the ad-GFP was more than the ad-CRE, $^{*}P < 0.01$; and for Myogenin, the ad-GFP was more than the ad-CRE, $^{***}P < 0.001$. *(D)* The ad-CRE and ad-GFP groups were stained with ALP, respectively. *(E)* The expression of ALP in the ad-CRE was significantly lower than that in the ad-GFP, $^{**}P < 0.01$. *(F)* RT-PCR results showed that in the ad-CRE group, the downstream primer TCF1 of β-catenin decreased significantly, $^{*}P < 0.05$; osteogenesis-related genes Runx2, osteopontin, and col1 were also significantly lower than the ad-GFP group, $^{**}P < 0.01$; in the ad-GFP group, myogenic-related genes MyoD, Myf5, and MEF2C were higher than the ad-CRE group, $P < 0.05$. *(G)* Based on the two groups, DMSO and osthole were used to intervene for 72 h, and ALP staining was observed.

DOI: 10.1002/jcsm.12938

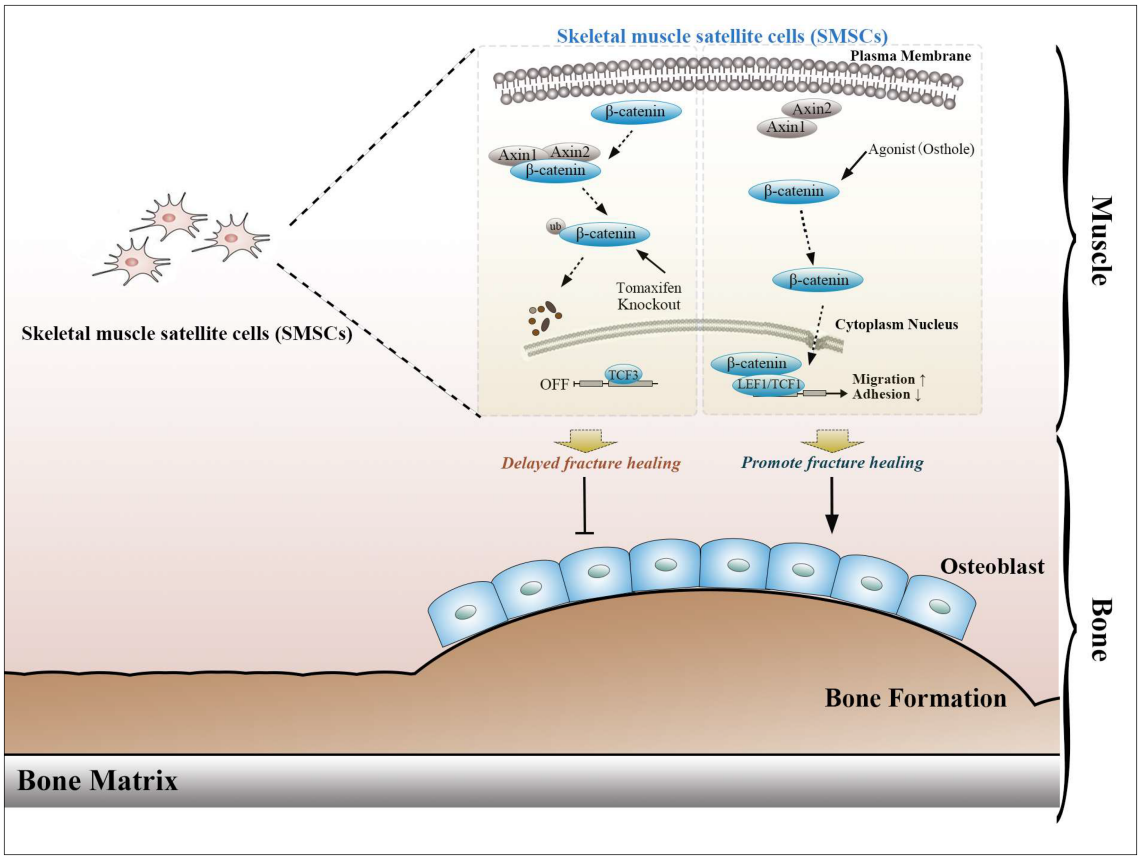

Figure 6 Skeletal muscle satellite cells play a vital role in the healing of osteoporotic fractures mediated by β-catenin. When β-catenin is knocked out in SMSCs, fracture delay can occur. On the contrary, when β-catenin is promoted, fracture healing can be promoted.

last decade. Especially nitrogen bisphosphonates are the most commonly used and most affordable drug. The drugs have adverse effects, causing widespread concern.[37] However, these agents have shown adverse cardiovascular events in clinical trials.[38] From the perspective of the complexity of treatment and poor prognosis, the hospital cost with the highest OPFs each year is up to $5.1 billion.[39] Therefore, it brings pain and suffering, accompanied by the loss of function and quality of life and the risk of shortened life expectancy.

In summary, this study demonstrated that the coupling relationship between cells promoted the osteogenic differentiation of SMSCs to a certain extent, causing the migration of SMSCs to the fracture site and thus promoting repair. Moreover, the β-catenin signalling pathway plays a vital role, regulated the activities of chondrocytes and osteoblasts, and maintaining a balance between osteogenesis and osteoclast. On the contrary, after the knockout of the β-catenin of SMSCs, not only the myogenic differentiation decreased, but the osteogenic differentiation also decreased. The most serious thing was the destruction of bone mass and bone microstructure, and delayed fracture healing occurred. Future studies should focus on optimizing the research on mobilizing autologous stem cells to treat bone diseases and provide a scientific basis for clinical application.

Acknowledgements

This study was sponsored by research grants from the National Key R&D Program of China (2018YFC1704300), the National Natural Science Foundation of China (81973883), the Shanghai Scientific Research Project (19ZR1458000), the first round of a three-year Action Plan to Promote Clinical Skills and Clinical Innovation in Municipal Hospitals (16CR1017A), the Shanghai Traditional Chinese Medicine Medical Center of Chronic Disease (2017ZZ01010), the 'Innovation Team' development projects (IRT1270), and the Three-Year Action to Accelerate the Development of Traditional Chinese Medicine Plan [ZY(2018-2020)-CCCX-3003]. The authors certify that they comply with the ethical guidelines for authorship and publishing of the *Journal of Cachexia, Sarcopenia and Muscle*.

Conflict of interest

The authors declare that they have no conflict of interest.

References

1. Compston JE, Mcclung MR, Leslie WD. Osteoporosis. *Lancet* 2019;**393**:364–376.
2. Neugebauer J, Heilig J, Hosseinibarkooie S, Ross BC, Mendoza-Ferreira N, Nolte F, et al. Plastin 3 influences bone homeostasis through regulation of osteoclast activity. *Hum Mol Genet* 2018;**27**: 4249–4262.
3. Center JR, Bliuc D, Nguyen TV, Eisman JA. Risk of subsequent fracture after low-trauma fracture in men and women. *JAMA* 2007;**297**:387–394.
4. Xie Y, Zhang L, Xiong Q, Gao Y, Ge W, Tang P. Bench-to-bedside strategies for osteoporotic fracture: from osteoimmunology to mechanosensation. *Bone Res* 2019;**7**:25.
5. Bhandari M, Einhorn TA, Guyatt G, Schemitsch EH, Zura RD, Sprague S, et al. Total hip arthroplasty or hemiarthroplasty for hip fracture. *N Engl J Med* 2019;**381**: 2199–2208.
6. NIH Consensus Development Panel On Osteoporosis Prevention DAT. Osteoporosis prevention, diagnosis, and therapy. *JAMA* 2001;**285**:785–795.
7. Liu N, Garry GA, Li S, Bezprozvannaya S, Sanchez-Ortiz E, Chen B, et al. A Twist2-dependent progenitor cell contributes to adult skeletal muscle. *Nat Cell Biol* 2017;**19**:202–213.
8. Scott RW, Arostegui M, Schweitzer R, Rossi F, Underhill TM. Hic1 defines quiescent mesenchymal progenitor subpopulations with distinct functions and fates in skeletal muscle regeneration. *Cell Stem Cell* 2019; **25**:797–813.
9. Gunther S, Kim J, Kostin S, Lepper C, Fan CM, Braun T. Myf5-positive satellite cells contribute to Pax7-dependent long-term maintenance of adult muscle stem cells. *Cell Stem Cell* 2013;**13**:590–601.
10. Braun T, Gautel M. Transcriptional mechanisms regulating skeletal muscle differentiation, growth and homeostasis. *Nat Rev Mol Cell Biol* 2011;**12**:349–361.
11. Wada MR, Inagawa-Ogashiwa M, Shimizu S, Yasumoto S, Hashimoto N. Generation of different fates from multipotent muscle stem cells. *Development* 2002;**129**: 2987–2995.
12. Anderson JE, Do MQ, Daneshvar N, Suzuki T, Dort J, Mizunoya W, et al. The role of semaphorin3A in myogenic regeneration and the formation of functional neuromuscular junctions on new fibres. *Biol Rev Camb Philos Soc* 2017;**92**:1389–1405.
13. Marg A, Escobar H, Karaiskos N, Grunwald SA, Metzler E, Kieshauer J, et al. Human muscle-derived CLEC14A-positive cells regenerate muscle independent of PAX7. *Nat Commun* 2019;**10**:5776.
14. Rudolf A, Schirwis E, Giordani L, Parisi A, Lepper C, Taketo MM, et al. β-Catenin activation in muscle progenitor cells regulates tissue repair. *Cell Rep* 2016;**15**: 1277–1290.
15. Aloysius A, Dasgupta R, Dhawan J. The transcription factor Lef1 switches partners from beta-catenin to Smad3 during muscle stem cell quiescence. *Sci Signal* 2018;**11**. https://doi.org/10.1126/scisignal.aan3000
16. Suzuki A, Minamide R, Iwata J. WNT/β-catenin signaling plays a crucial role in myoblast fusion through regulation of nephrin expression during development. *Development* 2018;**145**:v168351. https://doi.org/10.1242/dev.168351
17. Slimani L, Vazeille E, Deval C, Meunier B, Polge C, Dardevet D, et al. The delayed recovery of the remobilized rat tibialis anterior muscle reflects a defect in proliferative and terminal differentiation that impairs early regenerative processes. *J Cachexia Sarcopenia Muscle* 2015;**6**: 73–83.
18. Li S, Liu D, Fu Y, Zhang C, Tong H, Li S, et al. Podocan promotes differentiation of bovine skeletal muscle satellite cells by regulating the Wnt4-β-catenin signaling pathway. *Front Physiol* 2019;**10**:10.
19. Chen D, Tang J, Wan Q, Zhang J, Wang K, Shen Y, et al. E-Prostanoid 3 receptor mediates sprouting angiogenesis through suppression of the protein kinase A/β-catenin/Notch pathway. *Arterioscler Thromb Vasc Biol* 2017;**37**:856–866.
20. Tang D, Hou W, Zhou Q, Zhang M, Holz J, Sheu T, et al. Osthole stimulates osteoblast differentiation and bone formation by activation of β-catenin-BMP signaling. *J Bone Miner Res* 2010;**25**:1234–1245.
21. Yun C, Wu S, Xin-Xin Z, Yan-Die L, Hao C, Hao LI. Osthole prevents acetaminophen-induced liver injury in mice. *Acta Pharmacol Sin* 2018;**39**:74–84.
22. Zhou Y, Wang J, Guo Y, Liu X, Liu S, Niu X, et al. Discovery of a potential MCR-1 inhibitor that reverses polymyxin activity against clinical *mcr-1*-positive *Enterobacteriaceae*. *J Infect* 2019;**78**:364–372.
23. Livak KJ, Schmittgen TD. Analysis of relative gene expression data using real-time quantitative PCR and the $2^{-\Delta\Delta CT}$ method. *Methods* 2001;**25**:402–408.
24. Yao L, Yang Y, He G, Ou C, Wang L, Liu K. Global proteomics deciphered novel-function of osthole against pulmonary arterial hypertension. *Sci Rep* 2018;**8**: 5556.
25. Goldring K, Partridge T, Watt D. Muscle stem cells. *J Pathol* 2002;**197**:457–467.
26. Fink B, Neuen-Jacob E, Lienert A, Francke A, Niggemeyer O, Ruther W. Changes in canine skeletal muscles during experimental tibial lengthening. *Clin Orthop Relat Res* 2001;**385**:207–218.
27. Sambasivan R, Yao R, Kissenpfennig A, Van Wittenberghe L, Paldi A, Gayraud-Morel B, et al. Pax7-expressing satellite cells are indispensable for adult skeletal muscle regeneration. *Development* 2011;**138**: 3647–3656.
28. Ding K, Liu WY, Zeng Q, Hou F, Xu JZ, Yang Z. Msx1-modulated muscle satellite cells retain a primitive state and exhibit an enhanced capacity for osteogenic differentiation. *Exp Cell Res* 2017;**352**: 84–94.
29. Judson RN, Quarta M, Oudhoff MJ, Soliman H, Yi L, Chang CK, et al. Inhibition of methyltransferase Setd7 allows the in vitro expansion of myogenic stem cells with improved therapeutic potential. *Cell Stem Cell* 2018;**22**:177–190.
30. Jin ZX, Liao XY, Da WW, Zhao YJ, Li XF, Tang DZ. Osthole enhances the bone mass of senile osteoporosis and stimulates the expression of osteoprotegerin by activating beta-catenin signaling. *Stem Cell Res Ther* 2021;**12**:154.
31. Meng Y, Lin T, Jiang H, Zhang Z, Shu L, Yin J, et al. miR-122 exerts inhibitory effects on osteoblast proliferation/differentiation in osteoporosis by activating the PCP4-mediated JNK pathway. *Molecular Therapy - Nucleic Acids* 2020;**20**:345–358.
32. Ono Y, Calhabeu F, Morgan JE, Katagiri T, Amthor H, Zammit PS. BMP signalling permits population expansion by preventing premature myogenic differentiation in muscle satellite cells. *Cell Death Differ* 2011;**18**:222–234.
33. Liu H, Liu Z, Du J, He J, Lin P, Amini B, et al. Thymidine phosphorylase exerts complex effects on bone resorption and formation in myeloma. *Sci Transl Med* 2016;**8**: 113r–353r.
34. Black DM, Rosen CJ. Clinical practice. Postmenopausal osteoporosis. *N Engl J Med* 2016;**374**:254–262.
35. Brauer CA, Coca-Perraillon M, Cutler DM, Rosen AB. Incidence and mortality of hip fractures in the United States. *JAMA* 2009;**302**:1573–1579.
36. Banks E, Beral V, Reeves G, Balkwill A, Barnes I. Fracture incidence in relation to the pattern of use of hormone therapy in

postmenopausal women. *JAMA* 2004;**291**: 2212–2220.
37. Leder BZ, Clarke BL, Shane E, Khosla S, Kiel DP. A lot of progress, with more to be done: a response to NIH pathways to prevention report "Research gaps for long-term drug therapies for osteoporotic fracture prevention". *J Bone Miner Res* 2019;**34**:1549–1551.
38. Mullard A. Merck & Co. drops osteoporosis drug odanacatib. *Nat Rev Drug Discov* 2016;**15**:669.
39. Singer A, Exuzides A, Spangler L, O'Malley C, Colby C, Johnston K, et al. Burden of illness for osteoporotic fractures compared with other serious diseases among postmenopausal women in the United States. *Mayo Clin Proc* 2015;**90**:53–62.